An electrochemical and XPS study of Ag–Pb binary alloys incorporated in Nafion® coatings

I.G. CASELLA

Dipartimento di Chimica, Universita' degli Studi della Basilicata, Via N. Sauro 85, 85100 Potenza, Italy

Abstract

Glassy carbon electrodes coated with thin films of Nafion® metalized with silver and lead species were investigated by cyclic voltammetry, chronoamperometry and X-ray photoelectron spectroscopy (XPS). Metalization of Nafion® film was accomplished by dipping the coated electrodes in 3 mM $AgNO_3$ + 3 mM $Pb(NO_3)_2$ solution for 10 min. The resulting chemically modified electrodes were electrochemically characterized toward the oxidation of amino compounds in carbonate solutions buffered at pH 10. Under chronoamperometric experiments carried out at a constant applied potential of 0.95 V vs SCE, the linear range ($r^2 > 0.995$) was determined to be at least three decades and the limit of detection range from 26 μM (ethylamine) and 65 μM (*tert*-butylamine), for the investigated amino compounds. The perm-selective properties of the Nafion® film with respect to anion species were investigated toward the electrooxidation of ethylamine in presence of large concentration of chloride ions. The XPS analysis revealed heterogeneous distribution of the catalytic species dispersed in the metalized Nafion® film. Thus, a comparison of the spectra of Ag3d and Pb4f acquired at various take-off angles, indicates an increase in the atomic ratio Ag:Pb and a notable enrichment of lead oxide species in the outer surface of the film when compared with the bulk membrane coated electrode.

1. Introduction

Various methods for the separation and quantification of amines by high-performance liquid chromatography have recently been proposed [1–3]. Derivatization of the amino group has often been undertaken in order to increase the analytical sensitivity of the proposed method, since these compounds do not have any adequate chromophore and/or flourophore groups, so that the traditional spectrophotometric detector cannot be used for low concentration levels. Thus, *o*-phthalaldehyde, dansyl chloride, benzoyl chloride, fluorescamine, 4-chloro-7-nitro-benzofurazane and other compounds were used as pre- or post-column derivatizing reagents [4–6] in fluorescence and UV–visible detection mode.

Direct electrochemical methods are very sensitive and selective techniques for the determination of many important electroactive molecules such as carbohydrates [7–11], alcohols and alditols [12], *n*-alkanolamines [13], amino acids and sulfur-containing compounds [14–17]. However, electrochemical determinations are difficult at ordinary carbon or noble metal electrodes due to the large oxidation overpotential and severe fouling effects caused by adsorption of reaction products or interfering species on the electrode surface. A promising approach for minimizing overvoltage and

fouling effects is through the use of novel electrode materials and chemically modified electrodes (CMEs). These electrodes are generally prepared by dispersion of a specific redox mediator onto or within a suitable electrodic support. The main functions of the support are to separate the particles physically in order to diminish the rate of their degradation by agglomeration, and to increase the active surface area of the redox mediator. Generally, the modification of traditional electrode surfaces provides an efficient way of confining active catalytic particles to the effective spatial region, and combines the experimental advantages of heterogeneous catalysis with the benefits of a three-dimensional distribution of the catalytic centres typically characteristic of homogeneous catalysis. Thus several strategies to prepare CMEs have been suggested either by incorporation of redox catalyst in carbon paste matrices [18–20], electrodeposition of Prussian blue films and their metals analogues [21–23], or direct electrodeposition of oxide–hydroxide films of transition metals on inert electrode substrate [24, 25]. During the last two decades some fundamental investigations were undertaken on the catalysis of several electrochemical reactions on metal substrates modified by heavy metal adatoms by codeposition processes or by melting the appropriate pure metal powders [26, 27]. Thus, alloys or heavily-doped substrates were used as electrode

materials for the oxidation of alcohols [28–30], carbo-hydrates [31–34], formic acid [30, 35], sulfur-containing compounds [36, 37] and amines [38–40]. The presence of an alloying metal either: (i) modifies the electronic and physical structure of the electrode surface, (ii) blocks the poison formation reactions or (iii) adsorbs oxygen/hydroxyl ions which can take part in the main oxidation reaction.

One approach to achieve stabilization of active metals catalyst during the electrooxidation process involves their incorporation in inert or electroactive polymeric matrices. The dispersion of metal particles into a polymer matrix provides the possibility of high specific areas of metal catalyst and, thus, improved catalytic efficiency. Very often, polymeric membranes are used as size and/or charge exclusion barriers in order to improve selectivity and to prevent fouling effects of the CMEs. Thus, electrodes modified by a suitable polymer matrix such as polyaniline and polypyrrole incorporating metal-complex species have been characterized and proposed for the oxidation of several electroactive molecules [41–45]. One of the most widely studied polymer matrix is Nafion®, a perfluoronated polysulf-onate ion-exchange polyelectrolyte. This is due to its good chemical, electrochemical and thermal stability, hydrophilic character and good transport properties, in addition to being commercially available in solution and membrane form. Moreover, the hydrophilic negatively charged sulphonato group in Nafion® enables it selec-tively to incorporate cations by electrostatic interaction. Extensive fundamental studies have been made on the dynamics of charge, mass transport and thermodynam-ics of ion-exchange reactions [46–49]. Thus, CMEs prepared by incorporation of transition metals onto and within Nafion® films were widely characterized and used as electrochemical sensors for the analytical deter-mination in batch and flowing systems of several electroactive molecules [50–54].

In this work a Nafion® membrane metalized with Ag and Pb particles was characterized as a chemically modified electrode (Naf/Ag–Pb) towards the elect-rooxidation of aliphatic amines in carbonate solution buffered at pH 10. Electrochemical and X-ray photo-electron spectroscopy (XPS) techniques were used to characterize the CME.

2. Experimental details

2.1. Reagents

Solutions were prepared from analytical-reagent grade chemicals without further purification and by using twice distilled and deionized water. Sodium carbonate, sodium hydrogen carbonate, $AgNO_3$ 99 + %, $Pb(NO_3)_2$ 99 + % and aliphatic amines were purchased from Aldrich-Chemie. Glassy carbon substrates used for the XPS investigation were obtained from HTW (Hoch-Temperatur-Werkstoffe, Meitingen, Germany).

2.2. Apparatus

A model 273 Princeton Applied Research (PAR EG&G) potentiostat/galvanostat was used for electrochemical measurements. Cyclic voltammetry (CV) was done in a three-electrode cell using the Naf/Ag–Pb as working electrode, a SCE (4 M KCl) reference electrode and a platinum foil counter-electrode. The glassy carbon electrode (0.125 cm^2 geometric area) used in CV was purchased from PAR. All current densities are quoted in mA cm^{-2} of the apparent geometric area of substrate electrode. All experiments were carried out at ambient temperature.

X-ray photoelectron spectra were collected using a Leybold LH X1 spectrometer using nonmonochroma-tized MgK_α radiation (1253.6 eV) operating at 13 kV and 20 mA as an excitation source. The binding energy (BE) scale was calibrated with respect to the $Cu2p_{3/2}$ (932.7 eV, with a full-width at half-maximum (FWHM) of 1.75 eV) and $Au4f_{7/2}$ (84.0 eV with a FWHM of 1.20 eV) signals. Spectra were recorded only after the wide scan showed that no features arose from the copper tape and from the sample rod. Wide and detailed spectra were collected in fixed analyser transmission (FAT) mode with a pass energy of 50 eV and a channel width of 1.0 and 0.1 eV, respectively. The vacuum in the analysis chamber was always better than 5×10^{-9} mbar.

Data acquisition and spectra analysis were accom-plished using a data processing program [55]. Satellites and a nonlinear Shirley background were substracted from the spectrum before curve fitting analysis. Assum-ing a homogeneous chemical composition of the elec-trode surface, the elemental surface stoichiometries were obtained from peak area ratios corrected by sensitivity factors derived by Wagner [56], where the atomic sensitivity factors are based on calculated cross-section corrected for the kinetic energy dependence of the spectrometer detection efficiency and the average value for the dependence of the mean free path of the photoelectron in the sample on kinetic energy. Gauss-ian–lorenzian sum functions were used to fit the detailed regions. The gaussian–lorenzian (GL) mixing ratio and the FWHM of O1s peaks were the same as in previous studies on carbon-, platinum- or nickel-oxygen com-pounds [24, 25].

All samples, after preparation, were washed thor-oughly with bidistilled water and dried before executing the spectroscopic analysis.

2.3. Electrode preparation

Prior to modification, the glassy carbon electrodes were polished with 0.05 μm α-alumina powder on a polishing microcloth and washed with twice distilled water. A Nafion® membrane was cast over the working electrode by spreading a thin layer of 10 μL of 1% Nafion®/ethanol + water solution (solution prepared from Naf-ion® 117, molar mass 1100 g purchased from Aldrich) and allowing the solvent to evaporate for 10 min in an

air oven at about 50 °C, so that a uniform film was formed over the entire electrode surface. The resulting thickness of the film was estimated from the volume and density of the Nafion® membrane to be about 0.8–1.5 μm. The Nafion® films were metalized by dipping the coated electrodes in 3 mM AgNO$_3$ + 3 mM Pb(NO$_3$)$_2$ solution for 10 min. The modified electrodes were rinsed thoroughly with distilled water before the successive use.

Ag–Pb oxide films also were prepared by anodic electrodeposition on the glassy carbon electrode (0.95 V, 30 min) from buffer 20 mM Na$_2$CO$_3$/NaHCO$_3$ solution at pH 10 containing 5 mM AgNO$_3$ and 5 mM Pb(NO$_3$)$_2$.

3. Results and discussion

3.1. *Electrochemical characterization*

Figure 1 shows cyclic voltammograms of a Naf/Ag–Pb electrode in 20 mM Na$_2$CO$_3$/NaHCO$_3$ solution buffered at pH 10 in the presence of 8 mM ethylamine. For comparison the voltammograms of the Naf/Ag and Naf/Pb electrode are also reported. The metalation of the Nafion® membrane in Naf/Ag and Naf/Pb electrode was obtained by soaking the coated electrode for 10 min in 5.0 mM AgNO$_3$ and 5.0 mM Pb(NO$_3$)$_2$ solution, respectively. The surface composition of the Ag–Pb alloy in the Nafion® film was calculated by XPS data (see below). Although silver- and lead-based electrodes show catalytic activities towards the electrocatalytic oxidation of ethylamine (Figure 1), the direct interaction of silver and lead particles in the Nafion® film gives a synergistic effect on the kinetic electrooxidation of the amino compounds. Thus, a Nafion® coated electrode with a percent metal composition of about 5% Ag and 95% Pb shows a notable increase in the oxidation current in the region of potential between 0.8 V and 1.0 V vs SCE. A similar behaviour was observed for other amino compounds investigated such as ammonia,
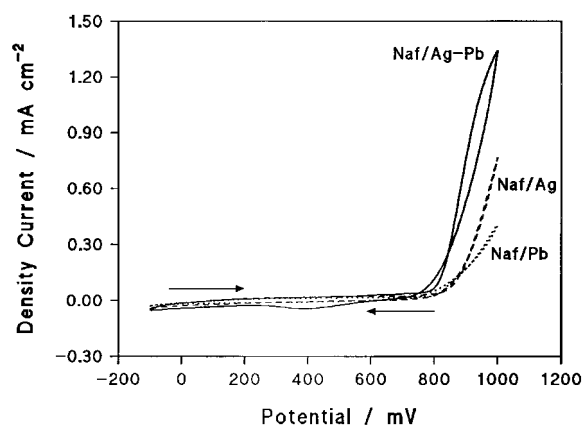
methylamine, 1-butylamine, *tert*-butylamine, trimethylamine, cadaverine and putrescine. As reported by Ge and Johnson [37, 38], the electrooxidative behaviour of aliphatic amines at Ag–Pb electrodes have been explained on the basis of a bifunctional action of the silver and lead particles, in which the analytes undergo preadsorption at the corresponding Ag species with the concomitant water discharge reaction occurring at adjacent PbO$_2$ sites. A similar electrochemical mechanism was postulated for Bi–PbO$_2$, Au–Ag, Pt–Ru, Pt–Bi and other alloy systems [26, 30, 40, 57]. In order to provide the effects of the Ag/Pb atomic ratio on the electrocatalytic activity towards amines oxidation, several Naf/Ag–Pb electrodes with various metallic composition were considered. Figure 2 shows the effect of metal film composition on the electrode performance. A maximum electrochemical activity toward ethylamine oxidation was observed for coated electrodes metalized in solutions containing 3 mM Ag$^+$ plus 3 mM Pb^{2+}. The relevant percent chemical composition of the metalized Nafion® film, evaluated by XPS analysis, was about 5% Ag$^+$ and 95% Pb^{2+}.

The effect of pH on the electrooxidation currents was investigated by cyclic voltammetry of 3.5 mM ethylamine solutions maintained at a constant ionic strength with 0.1 M NaClO$_4$. The pH was changed between 8 and 13. The oxidation currents in the potential range 0.8–1.1 V vs SCE showed a notable increase with increasing pH up to value of 10, while the net oxidation currents remained practically constant for pH between 11 and 13. The attenuation of the anodic currents for pH < 10 was explained on the basis of protonation of the amino compounds which are not electroactive in the protonated form [38–40]. It is interesting to observe that, on the Ag–Pb preanodized alloy electrodes [38, 39] a decrease in the ethylamine signal was also observed for pH > 11. This last behaviour was attributed to competitive
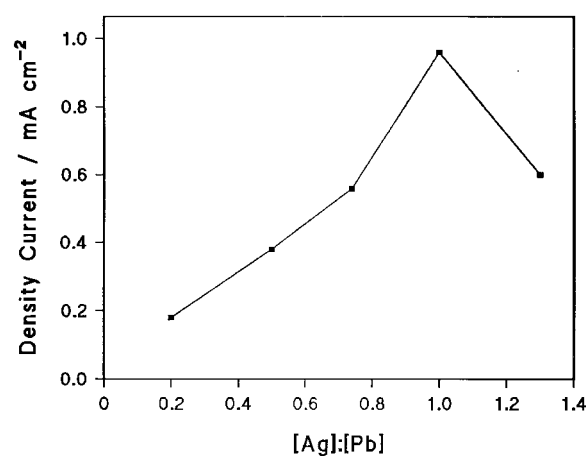
Fig. 1. Cyclic voltammograms (10th cycle) of 8 mM ethylamine in 20 mM Na$_2$CO$_3$ + NaHCO$_3$ solution buffered at pH 10 at a Naf/Ag–Pb (5:95) electrode, Naf/Ag and Naf/Pb electrodes. Scan rate 50 mV s^{-1}.

Fig. 2. Dependence of the oxidation peak current on the concentration ratio between AgNO$_3$ and Pb(NO$_3$)$_2$ in the dipping solution. In all cases the AgNO$_3$ was 3 mM. The coated Nafion® electrode were metaled in the resulting solution for 10 min of immersion time. Values of currents were evaluated by cyclic voltammograms as in Figure 1 measuring the currents at 0.95 V in buffer carbonate solutions containing 5 mM ethylamine.

adsorption by hydroxyl ions for the silver catalytic sites. Alternatively, it is possible that stable silver oxide formation (i.e., Ag_2O, AgO), through increasing pH, deactivates the catalytic centres. Thus, the unchanged electrode performance of the Naf/Ag–Pb electrode observed for pH values higher than 10, can be explained because, at the modified electrode, OH^- ions can be preferentially expelled from the negatively charged Nafion® membrane by electrostatic repulsion.

Typical chronoamperometric responses (I/t curves) obtained at a Naf/Ag–Pb electrode as a function of standard addition of ammonia (A), ethylamine (B) and 1-buthylamine (C) into well-stirred solutions (500 rpm) are shown in Figure 3. The curves were recorded for a constant applied potential of 0.95 V vs SCE. Linear ranges, limits of detection and sensitivity factor for several amino compounds, obtained by chronoamperometric analysis, are summarized in Table 1. Generally the linear range ($r^2 > 0.995$) was determined to be at least three decades for the amines and the limit of detection ranged from 26 μM for ethylamine and 65 μM for *tert*-butylamine. To a first approximation, molar sensitivities related to the molecular size of the amines and steric hyndrance of the amino group at the catalytic sites. In contrast, with the decreased molar sensitivity in the order primary > secondary > tertiary amines observed at a nickel-modified electrode [58], in the case of the Naf/Ag–Pb electrode the molar sensitivity of the trimethylamine is comparable with those obtained with ethylamine and diethylamine (see Table 1).

To evaluate the protective properties of the Nafion® membrane by chloride ions, chronoamperometric measurements of the ethylamine electrooxidation in the presence of chloride ions were performed at the Naf/Ag–Pb electrode and, as comparison, at the Ag–Pb electrodeposited alloy on glassy carbon. Figures 4 and 5 shown the effect of increasing chloride concentration on

Table 1. Chronoamperometric analysis of amino-containing compounds at the Naf/Ag–Pb electrode

Compound	LOD /μM	Linear range /mM	Sensitivity /μA (mM^{-1})
Ammonia	27	0.027–12	18.4
Ethylamine	26	0.026–11	12.8
1-butylamine	39	0.055–9	9.8
Diethylamine	38	0.055–10	9.3
Trimethylamine	41	0.041–10	9.5
tert-Butylamine	65	0.065–8	2.6
Putrescine	56	0.056–9	7.9
Spermidine	58	0.058–9	7.1

Chronoamperometric measurements obtained with a Naf/Ag–Pb electrode prepared as reported in the experimental section (Section 2). Electrolyte: 20 mM $Na_2CO_3/NaHCO_3$ solution buffered at pH 10; applied potential: 0.95 V vs SCE; rotation of the magnetic bar: 500 rpm.

the oxidation current of ethylamine for a Naf/Ag–Pb electrode and an Ag–Pb alloy electrodeposited film, respectively. About 90% of the response was lost for the Ag–Pb alloy electrode at a Cl^- concentration of about 35 mM (see Figure 5). In particular, the Ag–Pb electrodeposited alloy, shows a dramatic diminution of the amperometric signal (about 72%) after an initial addition of 5 mM Cl^-. In contrast, the Nafion® coated electrode preserves most of its initial response with increasing chloride concentration. In the case of Naf/Ag–Pb electrode, about 28% of the response was lost at a chloride concentration of 55 mM. Thus Nafion®, in the form of a cation-exchange polymer membrane, is effective in selectively excluding anions from the electrode surface. The dramatic effect of chloride ions on the amperometric response was interpreted considering that Cl^- adsorbs favourably at silver sites with subsequent partial inhibition of the discharge of water, as well as amine adsorption at these sites [38]. The property of the Nafion® membrane, has previously
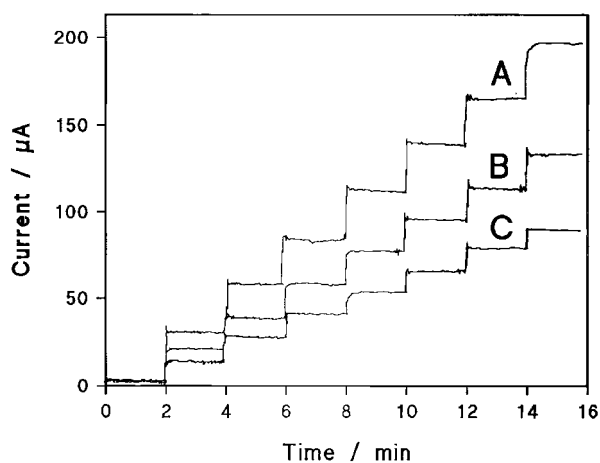

Fig. 3. Chronoamperometric measurements obtained on increasing concentrations in 1.5 mM steps of ammonia (A), ethylamine (B) and 1-butylamine (C) at a Naf/Ag–Pb electrode. Electrolyte: 20 mM Na_2CO_3 + $NaHCO_3$ solution buffered at pH 10; applied potential 0.95 V vs SCE; rotation of magnetic bar 500 rpm.
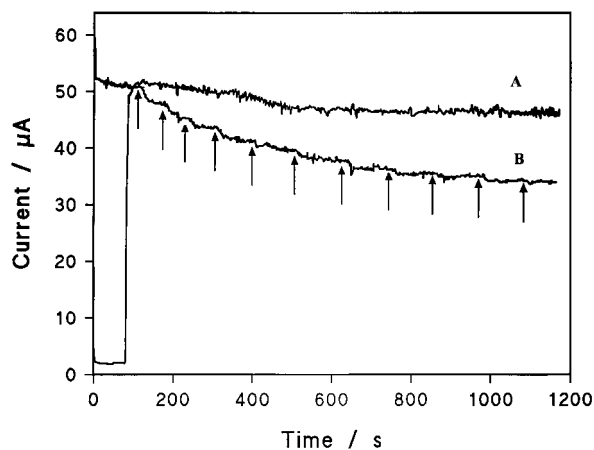

Fig. 4. Chronoamperometric measurements obtained with a Naf/Ag–Pb electrode in buffered carbonate solutions containing 5 mM ethylamine (A) and on increasing concentrations in 5 mM steps of Cl^- ions (B). Other experimental conditions as in Figure 3.
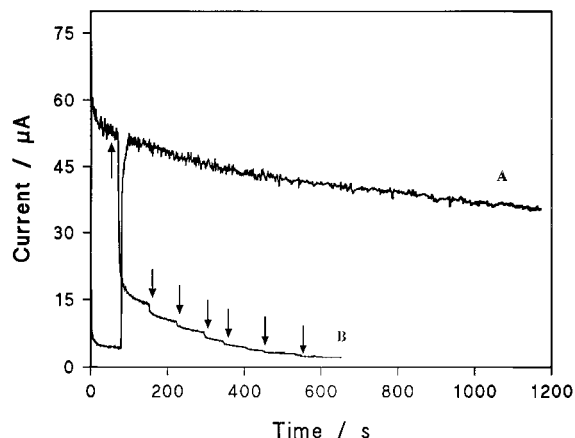
Fig. 5. Chronoamperometric measurements obtained with a Ag–Pb alloy film electrodeposited on the glassy carbon electrode. Conditions of electrode preparation are reported in Section 2. Other experimental conditions as in Figure 4.

been exploited for elimination of chloride and other common interferents in the electrochemical determination of carbohydrates in biological fluids [59, 60]. By comparison of the curves A in Figures 4 and 5, it can be observed that the chronoamperometric response of ethylamine obtained at Ag–Pb electrodeposited alloy on the glassy carbon substrate decayed by about 30% over about 20 min of operation time, while over the

same time a diminution of the amperometric signal of about 11% on the Naf/Ag–Pb electrode was observed. Nevertheless, a large concentration of Na^+ in the supporting electrolyte (i.e., higher than 100 mM) induces an exchange in the Ag^+ and Pb^{2+} ions from the polymer film. Thus, the Nafion® film used under the present experimental conditions, acts as a protective membrane either to prevent interference effects by fouling species or to avoid dissolution of the silver and lead species from the electrode surface.

3.2. *XPS Measurements*

To understand the effects of electrochemical conditioning in buffer carbonate media on the electroactivity and chemical composition of the Ag–Pb microparticles dispersed in the polymer matrix, XPS was employed as an analytical surface technique. Throughout this work, Pb4f, Ag3d, O1s, F1s, and Na1s regions were collected and analysed for each specimen. A shift between 3.5 and 4.5 eV due to sample charging was observed in all XPS lines. The binding energy axis origin in all figures was not corrected for surface charging, but peak positions (BE) in the text are corrected by referring to the Na1s peak after setting its BE to 1071.4 eV [61]. To determine the chemical composition of the electroactive species and to check the homogeneity of the metalized Nafion®
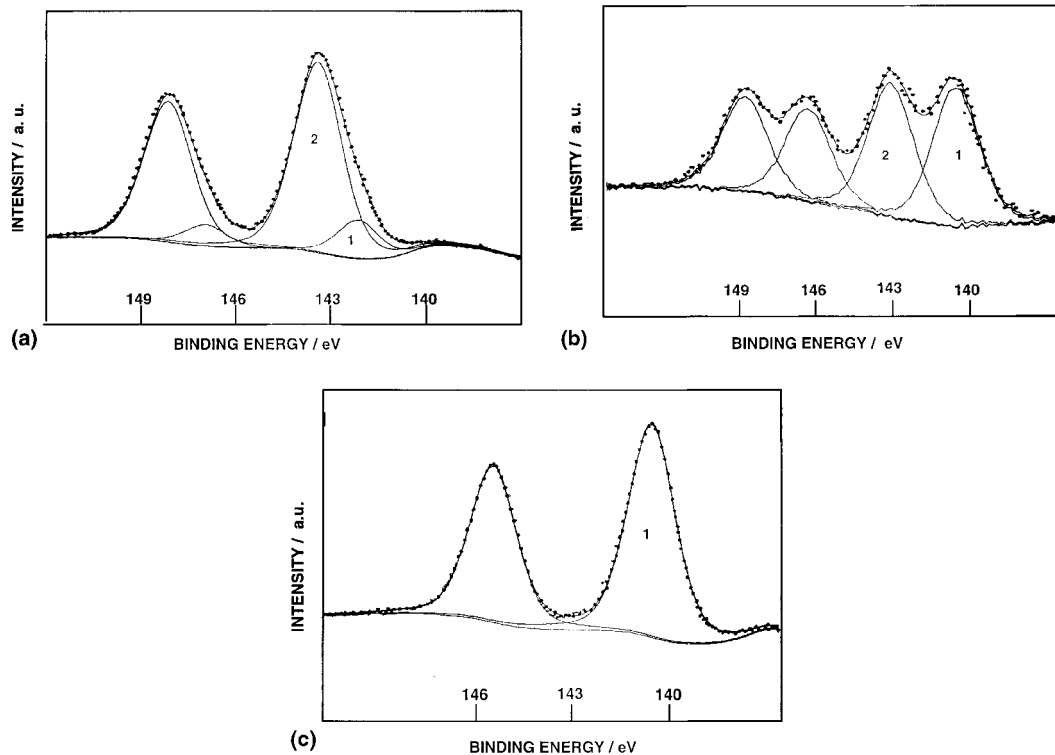

Fig. 6. (a) XP detailed spectra of the Pb4f region taken at 90° take-off angle of a Naf/Ag–Pb electrode obtained by dipping the coated Nafion® electrode in 3 mM $AgNO_3$ and 3 mM $Pb(NO_3)_2$ solution for 10 min. Modified electrode treated electrochemically in 20 mM Na_2CO_3 + $NaHCO_3$ solution buffered at pH 10 by cycling continuously (30 cycles) the potential between −0.1 and 1.0 V vs SCE. Electrode washed thoroughly with water and dried before executing spectroscopic analysis. (b) XP detailed spectra of the Pb4f region taken at 30° take-off angle relevant to the electrode analysed in Figure 6(a). (c) XP spectra of the Pb4f region taken at 90° take-off angle of an Ag–Pb alloy film prepared by anodic electrodeposition on the glassy carbon electrode (0.95 V, 30 min) from buffer 20 mM Na_2CO_3/$NaHCO_3$ solution at pH 10 containing 5 mM $AgNO_3$ and 5 mM $Pb(NO_3)_2$. Resulting electrode was treated electrochemically as in Figure 6(a).

film, XPS depth profiling of selected samples was performed. The Pb4f spectrum taken at a 90° and 30° inclination angles (take-off angle, ϕ) of the Naf/Ag–Pb electrode after electrochemical treatment in carbonate buffer solution by cycling the potential (30 cycles) between −0.1 and 1.0 V vs SCE are shown in Figure 6(a) and (b), respectively. For curve fitting analysis, a spin-orbit splitting of 4.9 eV and a $4f_{5/2}$:$4f_{7/2}$ peak area ratio of about 0.75 were fixed for each doublet considered [61]. Figure 6(a), taken at a 90°, shows a two spin-orbit doublet, with well resolved $Pb4f_{7/2}$ peaks at 138.8 ± 0.4 eV and 137.5 ± 0.4 eV of BE. The large peak at 138.8 eV, in agreement with literature data [61], can be assigned to Pb^{2+} bonded with sulfonate groups of the Nafion® film. The peak centred at 137.5 eV is assigned to lead oxides species (i.e., PbO and/or PbO_2) [61–64]. Unfortunately, the exact assignment of the lead oxides is ambiguous owing to little or no difference between the Pb4f binding energies of different lead oxide compounds. In addition, the correspondent Auger signals, have a complex structure, discouraging their use in systems involving lead compound species. However, in this work, the exact assignment is not essential. The peak at 137.5 eV was considered as a sum of PbO and PbO_2 contributions and indicated as PbO_x. It is interesting to compare Figure 6(a) with Figure 6(b) recorded at a 30° take-off angle. It is apparent that more lead oxide species (PbO_x) were found in the spectra obtained at 30°. The increase in the ratio of the lower to the higher binding energy component (R_{PbSO_3/PbO_x}) with decrease in take-off angle, indicates that more PbO_x is formed towards the outer layer of the metalized Nafion® film. As comparison, the Pb4f signal of Ag–Pb alloy, obtained by direct anodic electrodeposition on the glassy carbon substrate, shows a well resolved spin-orbit doublet with a $Pb4f_{7/2}$ peak at 137.8 eV of BE, which can be ascribed to lead oxide species (Figure 6(c)). These results, suggest that Nafion® film acts as a selective membrane with respect to OH⁻ ions avoiding the lead oxide formation in the bulk film. In consequence, the lead species entrapped in the polymer film are probably directly bonded by electrostatic interaction at the −SO_3^- sites of the membrane.
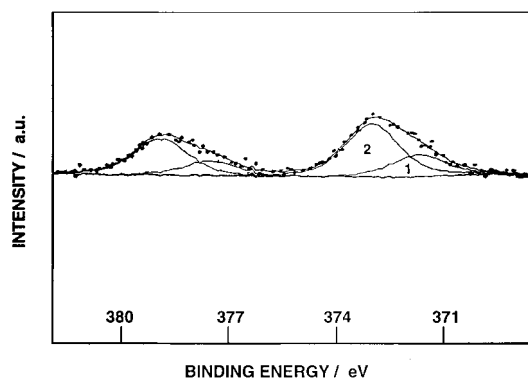

Fig. 7. XP spectra of the Ag3d region taken at 90° take-off angle relevant to the electrode analysed in Figure 6(a).

Typical XP spectra of the Ag3d signal of the Naf/Ag–Pb electrode after electrochemical treatment in carbonate buffer solution (by continuous cycling the potential between −0.1 and 1.0 V) is shown in Figure 7. A spin-orbit splitting of 6.0 eV and a $3d_{5/2}$:$3d_{3/2}$ peak area ratio of about 0.66 [61] was used for the curve fitting analysis. The figure shows generally two spin-orbit doublets, with $Ag3d_{5/2}$ peaks at 367.5 ± 0.4 eV and 368.4 ± 0.4 eV of BE, assigned to silver oxide species and metallic silver [38, 61, 65, 66], respectively. Unequivocal assignment of the oxide species based on the XPS signal position alone is not possible, because the Ag3d binding energies of AgO and Ag_2O are closely spaced. In addition, the full width at half maximum of 1.9 eV suggests the presence of more than one oxide component under the considered peaks. Thus, the peak at lower binding energy can be expected to consist of a mixture of Ag_2O and AgO species. In contrast to what is observed for the Pb4f signal, the peak shape of the Ag3d signal appears to be insensitive to take-off angle. In fact, an atomic ratio of 0.4 ± 0.1 between silver oxide species and Ag^0 was observed for all Naf/Ag–Pb electrodes analysed at various take-off angles.

Curve fitting of the O1s signal (not shown here), generally gives three contributions at 529.9 ± 0.3 eV, 531.5 ± 0.5 eV and 533.3 ± 0.5 eV which, on the basis of their BEs, were assigned to lattice oxide ions O^{2-}, hydroxide ions OH⁻ and/or cheto groups and atomic adsorbed oxygen species, alcohols groups and/or adsorbed water on the electrode surface, respectively [24, 25]. Nevertheless, in general, the specific assignment of the O1s peaks is more complex and ambiguous owing to uncertainty in the BEs values of the various oxygen species (i.e., oxygen–carbon and/or oxygen–metal species) and degree of disorder and roughness of the specific material surface considered. However, in this work, we are particularly concerned with the total oxygen content. Although the same line-shape of the O1s signal was obtained for various take-off angles, comparison of the O1s/F1s intensity ratio acquired at 90°, 60° and 30° shows enrichment of oxygen species in the outer surface relative to the bulk film coated electrode. This result is in agreement with the previous observation, where an enrichment of lead oxide species in the outer surface of the membrane was observed. Table 2 summarizes the binding energies and the atomic ratio of the silver and lead species found on the surface of the electrode electrochemically treated in buffer carbonate solutions. It is seen that the metalized Nafion® membrane shows heterogeneous chemical composition of the catalyst particles (i.e., Ag% and Pb%) between the bulk and surface film. In addition, the chemical surface composition of the electrode appears to be insensitive to particular electrochemical treatment and polarization. In particular, looking at Table 2, it is possible to make some considerations:

(i) the comparison of the Ag3d/Pb4f intensity ratio at various take-off angles, reveals an enrichment of silver on the surface film relative to bulk membrane.

Table 2. XPS data of Naf/Ag–Pb electrodes electrochemically treated in 20 mM Na_2CO_3/$NaHCO_3$ solution buffered at pH 10

	$Ag3d_{5/2}$ eV	$Pb4f_{7/2}$ eV	RAg_1/ Ag_2	RPb_1/ Pb_2	Ag:Pb
Naf/Ag–Pb*					
90°	367.5 (1) 368.4 (2)	137.4 (1) 138.8 (2)	0.30	0.11	Ag_5Pb_{95}
60°	367.6 368.5	137.5 138.6	0.28	0.17	Ag_9Pb_{91}
30°	367.4 368.6	137.6 138.9	0.33	1.0	$Ag_{18}Pb_{82}$
Naf/Ag–Pb†					
90°	367.5 368.6	137.6 138.8	0.25	0.17	Ag_6Pb_{94}
30°	367.7 368.4	137.7 138.8	0.21	1.1	$Ag_{21}Pb_{79}$
Naf/Ag–Pb‡					
90°	367.5 368.4	137.4 138.8	0.21	0.21	Ag_4Pb_{96}
30°	367.5 368.4	137.6 138.8	0.23	0.6	$Ag_{17}Pb_{83}$
Ag–Pb§					
90°	367.7 368.7	137.8	0.35		$Ag_{15}Pb_{85}$

* Naf/Ag–Pb electrode obtained by dipping the coated Nafion® film in 3 mM $AgNO_3$ + 3 mM $Pb(NO_3)_2$ solution for 10 min; the resulting electrode was electrochemically treated in buffer carbonate solution by continuous potential scanning (30 cycles) between 0.0 and 1.0 V vs SCE

† the same Naf/Ag–Pb electrode as (a) polarized at 0.95 V in buffer carbonate solution for 10 min

‡ the same Naf/Ag–Pb electrode as (a) polarized at 0.6 V in buffer carbonate solution for 10 min

§ Ag–Pb electrode obtained by anodic electrodeposition on the glassy carbon electrode (0.95 V, 30 min) from buffer 20 mM Na_2CO_3/ $NaHCO_3$ solution containing 5 mM $AgNO_3$ and 5 mM $Pb(NO_3)_2$. Ag:Pb represent the percentage atomic ratio between the Ag3d and Pb4f signals

In fact, the percent composition of the binary Ag–Pb alloy particles was about 5%:95% and 20%:80% at take-off angles of 90° and 30°, respectively;

(ii) The chemical composition of the silver species (i.e., R Ag$_1$/Ag$_2$) remains practically unchanged to sampling depths and is insensitive to electrochemical treatment of the Naf/Ag–Pb electrode in buffer carbonate solution;

(iii) In contrast, the chemical composition of the lead species (i.e., R Pb$_1$/Pb$_2$) dispersed in the polymer film changes with take-off angle. The R Pb$_1$/Pb$_2$ atomic ratio increases with decreasing take-off angle. This suggests an enrichment of lead oxides species in the film layer relative to the bulk Nafion® membrane. Moreover, as expected, the surface R Pb$_1$/Pb$_2$ atomic ratio increases with increasing applied potential. Thus, this result supports the view that polarization potentials higher than 0.6 V vs SCE induce the formation and stabilization of PbO and/or PbO_2 species at the electrode surface layer.

4. Conclusions

Dispersed silver–lead alloy in a Nafion® film has been investigated by cyclic voltammetry, chronoamperometry and XPS techniques. Electrochemical experiments have demonstrated that the Nafion/Ag–Pb electrode (with a percent chemical composition of 5% Ag and 95% Pb) shows excellent catalytic activity and good temporal stability toward the oxidation of amino compounds in carbonate solutions. The Nafion® film acts as a perm-selective cation-exchange polymer membrane, which prevents fouling caused by Cl$^-$ ions. Although the binding energies of Pb4f and Ag3d signals are closely spaced, by combining the XPS data of the resulting metalated Nafion films at various take-off angles, a consistent interpretation of the surface composition of the Naf/Ag–Pb electrodes has been given.

References

1. T. Matsumoto, T. Tsuda and O. Suzuki, *Trends Anal. Chem.* **9** (1990) 292.
2. I. Krause, A. Bockhardt, H. Neckermann, T. Henle and H. Klostermeyer, *J. Chromatogr. A* **715** (1995) 67.
3. N. Seiler and B. Knodgen, *J. Chromatogr.* **339** (1985) 45.
4. D.A Dobberpuhl, J.C. Hoekstra and D.C. Johnson, *Anal. Chim. Acta* **322** (1996) 55.
5. L.A. Allison, G.S. Mayer and R.E. Shoup, *Anal. Chem.* **58** (1984) 1089.
6. J. Steiner, H. Khalaf, W. Keese and M. Rimpler, *Anal. Chim. Acta* **327** (1996) 153.
7. R.D. Rocklin and C.A. Pohl, *J. Liq. Chromatogr.* **6** (1983) 1577.
8. T. Ueda, R. Mitchell, F. Kitamura and A. Nakamoto, *J. Chromatogr.* **591** (1992) 229.
9. D.C. Johnson and W.R. LaCourse, *Anal. Chem.* **62** (1990) 589A.
10. Y.C. Lee, *J. Chromatogr. A* **720** (1996) 137.
11. K. Kano, K. Takagi, K. Inoue, T. Ikeda and T. Ueda, *J. Chromatogr. A* **721** (1996) 53.
12. W.R. LaCourse, D.C. Johnson, M.A. Rey and W. Slingsby, *Anal. Chem.* **63** (1991) 134.
13. W.R. LaCourse, W.A. Jackson and D.C. Johnson, *Anal. Chem.* **61** (1989) 2466.
14. P. Luo, F. Zhang and R.P. Baldwin, *Anal. Chim. Acta* **244** (1991) 169.
15. D.C. Johnson, D. Dobberpuhl, R. Roberts and P. Vandeberg, *J. Chromatogr.* **640** (1993) 79.
16. P. Luo, F. Zhang and R.P. Baldwin, *Anal. Chem.* **63** (1991) 1702.
17. Y. Xie and C.O. Huber, *Anal. Chem.* **63** (1991) 1714.
18. P. Luo, S.V. Prabhu and R.P. Baldwin, *Anal. Chem.* **62** (1990) 752.
19. J. Wang, N. Naser, L. Agnes, H. Wu and L. Chen, *Anal. Chem.* **64** (1992) 1285.
20. J. Wang and N. Naser, *Anal. Chim. Acta* **316** (1995) 253.
21. J.A. Cox and P.J. Kulesza, *Anal. Chem.* **56** (1984) 1021.
22. K. Itaya, I. Uchida and V.D. Neff, *Acc. Chem. Res.* **19** (1986) 162.
23. J. Joesph, H. Gomathi and G. Prabhara Rao, *J. Electroanal. Chem.* **304** (1991) 263.

24. I.G. Casella, M.R. Guascito and M.G. Sannazzaro, *J. Electroanal. Chem.* **462** (1999) 202.
25. I.G. Casella and M.R. Guascito, *J. Electroanal. Chem.* **476** (1999) 54.
26. G. Kokkinidis, *J. Electroanal. Chem.* **201** (1986) 217.
27. R. Parsons and T. VanderNoot, *J. Electroanal. Chem.* **257** (1988) 9.
28. S. Swathirajan and Y.M. Mikhail, *J. Electrochem. Soc.* **138** (1991) 1321.
29. Y. Chen, K.Y. Chen and A.C.C. Tseung, *J. Electroanal. Chem.* **471** (1999) 151.
30. N.M. Markovic, H.A. Gasteiger, P.N. Ross Jr, X. Jiang, I. Villegas and M.J. Weaver, *Electrochim. Acta* **40** (1995) 91.
31. J.M. Marioli, P.F. Luo and T. Kuwana, *Anal. Chim. Acta* **282** (1993) 571.
32. P.F. Luo, T. Kuwana, D.K. Paul and P.M. Sherwood, *Anal. Chem.* **68** (1996) 3330.
33. G. Wittstock, A. Strubing, R. Szargan and G. Werner, *J. Electroanal. Chem.* **444** (1998) 61.
34. I.-H. Yeo and D.C. Johnson, *J. Electroanal. Chem.* **484** (2000) 157.
35. R. Schrebler, M.A. del Valle, H. Gómez, C. Veas and R. Córdova, *J. Electroanal. Chem.* **380** (1995) 219.
36. N.D. Popoviĉ and D.C. Johnson, *Electroanalysis* **11** (1999) 934.
37. M.E. Johll and D.C. Johnson, *Electroanalysis* **11** (1999) 534.
38. J. Ge and D.C. Johnson, *J. Electrochem. Soc.* **142** (1995) 1525.
39. J. Ge and D.C. Johnson, *J. Electrochem. Soc.* **142** (1995) 3420.
40. M.E. Johll, K.S. Asala, M. Swarts, J.W. Anderegg and D.C. Johnson, *Electroanalysis* **12** (2000) 248.
41. G. Tourillon and F. Garnier, *J. Phys. Chem.* **88** (1984) 5281.
42. K.M. Kost, D.E. Bartak, B. Kazee and T. Kuwana, *Anal. Chem.* **60** (1988) 2379.
43. W.T. Napporn, J.-M. Leger and C. Lamy, *J. Electroanal. Chem.* **408** (1996) 141.
44. I.G. Casella, T.R.I. Cataldi, A. Guerrieri and E. Desimoni, *Anal. Chim. Acta* **335** (1996) 217.
45. I. Becerik, Ş. Süzer and F. Kadirgan, *J. Electroanal. Chem.* **476** (1999) 171.
46. H.S. White, J. Leddy and A.J. Bard, *J. Am. Chem. Soc.* **104** (1982) 4811.
47. D.A. Buttry and F.C. Anson, *J. Am. Chem. Soc.* **105** (1983) 685.
48. M.S. Szentirmay, N. Prieto and C.R. Martin, *J. Phys. Chem.* **89** (1985) 3017.
49. A.R. Guadalupe, K.E. Liu and H.D. Abruña, *Electrochim. Acta* **36** (1991) 887.
50. L.D. Whiteley and C.R. Martin, *Anal. Chem.* **59** (1987) 1746.
51. J. Zhou and E. Wang, *Anal. Chim. Acta* **249** (1991) 489.
52. B.-T. Tay, K.P. Ang and H. Gunasingham, *Analyst* **113** (1988) 617.
53. K. Sugawara, S. Hoshi, K. Akatsuka and K. Shimazu, *J. Electroanal. Chem.* **414** (1996) 253.
54. I.G. Casella, M.R. Guascito, A.M. Salvi and E. Desimoni, *Anal. Chim. Acta* **354** (1997) 333.
55. E. Desimoni and U. Biader Ceipodor, *J Electron Spectrosc.* **56** (1991) 189.
56. C.D. Wagner, *Anal. Chem.* **51** (1979) 466.
57. N.D. Popovic, J.A. Cox and D.C. Johnson, *J. Electroanal. Chem.* **455** (1998) 153.
58. I.G. Casella, S. Rosa and E. Desimoni, *Electroanalysis* **10** (1998) 1005.
59. J.D. Harrison, R.F.B. Turner and H.P. Baltes, *Anal. Chem.* **60** (1988) 2002.
60. D.S. Bindra and G.S. Wilson, *Anal. Chem.* **61** (1989) 2566.
61. D. Briggs and M.P. Seah (Eds), 'Practical Surface Analysis', (J. Wiley, Chichester, UK, 1983).
62. L.R. Pederson, *J. Electron Spectrosc.* **28** (1982) 203.
63. J.A. Taylor and D.L. Perry, *J. Vac. Sci. Technol.* **A2** (1984) 771.
64. C. Malitesta, L. Sabbatini, P.G. Zambonin, L. Peraldo Bicelli and S. Maffi, *J. Chem. Soc., Faraday Trans.* **85** (1989) 1685.
65. V.K. Kaushik, *J. Electron Spectrosc.* **56** (1991) 273.
66. G.N. Salaita, Z.F. Hazos and G.B. Hoflund, *J. Electron Spectrosc.* **107** (2000) 73.